Feedback Regulation of Murine Autoimmunity via Dominant Anti-Inflammatory Effects of Interferon γ[1]

Alfredo Minguela,[2,3]* Silvia Pastor,[2,4]* Wentao Mi,* James A. Richardson,[†‡] and E. Sally Ward[5]*

There is a paucity of knowledge concerning the immunologic sequelae that culminate in overt autoimmunity. In the present study, we have analyzed the factors that lead to disease in the model of autoimmunity, murine experimental autoimmune encephalomyelitis (EAE). EAE in H-2^u mice involves autoreactive CD4$^+$ T cells that are induced by immunization with the immunodominant N-terminal epitope of myelin basic protein. The affinity of this epitope for I-A^u can be increased by substituting lysine at position 4 with tyrosine, and this can be used to increase the effective Ag dose. Paradoxically, high doses of Ag are poorly encephalitogenic. We have used quantitative analyses to study autoreactive CD4$^+$ T cell responses following immunization of mice with Ag doses that are at the extremes of encephalitogenicity. A dose of autoantigen that is poorly encephalitogenic results in T cell hyperresponsiveness, triggering an anti-inflammatory feedback loop in which IFN-γ plays a pivotal role. Our studies define a regulatory mechanism that serves to limit overly robust T cell responses. This feedback regulation has broad relevance to understanding the factors that determine T cell responsiveness. *The Journal of Immunology,* **2007, 178: 134–144.**

Murine experimental autoimmune encephalomyelitis (EAE)[6] is induced in susceptible strains of mice by immunization with autoantigen in adjuvant and is believed to be a representative model of multiple sclerosis in humans (1). Activated, autoreactive CD4$^+$ T cells enter the CNS where they can trigger infiltration of inflammatory leukocytes (2, 3). This leads to a cascade of events, including the up-regulation of MHC class II and adhesion marker expression on resident cells and the infiltration of macrophages, that culminate in the demyelination and paralysis that are characteristic features of EAE (2, 3).

In H-2^u mice, EAE is characterized by the induction of Th1-type cells that recognize the immunodominant N-terminal epitope of myelin basic protein (MBP1-9, acetylated at the N terminus) associated with the MHC class II molecule, I-A^u (4). MBP1-9 has a very low affinity for restricting MHC (5–7), and as a result, autoreactive T cells escape tolerance induction (8, 9). The affinity of the peptide for I-A^u can be increased at least 40- or 10^3-fold, respectively, by substituting lysine at position 4 of the peptide by alanine or tyrosine (7, 10). The molecular basis of this increase in affinity has recently become apparent from the solution of the x-ray structure of MBP1-9[4Y] (tyrosine at position 4) complexed with I-A^u (11).

Paradoxically, in earlier studies, the use of higher affinity position 4 analogs of MBP1-9 such as MBP1-9[4A] (alanine at position 4) or MBP1-9[4Y] as immunogens has been shown to be ineffective in inducing EAE (10, 12). By analyzing Ag-specific T cell lines that had been established in vitro using different Ag doses, binding by tetrameric, fluorescently labeled autoantigen complexes indicated that the higher Ag dose resulted in a population of lower avidity, autoantigen-specific T cells relative to those induced by encephalitogenic Ag doses (10). The residual, lower avidity T cells were proposed to be ineffective in eliciting disease. This is consistent with the concept from the NOD diabetes model that high-avidity (CD8$^+$) cells are more pathogenic than their lower avidity counterparts (13–15). However, highly avid MBP1-9:I-A^u-specific T cells do not induce disease following transfer into H-2^u mice (16), putting into question the correlation between avidity and pathogenicity. In addition, a recent study of MBP-induced EAE in SJL mice demonstrates that avidity maturation of Ag-specific T cells in the CNS does not occur, suggesting that T cells of a wide avidity spectrum participate in pathogenesis (17). Furthermore, in systems using foreign Ags such as cytochrome *c*, Ag dose has a limited impact on the avidity of the responding repertoire during the primary response provided that a threshold level is surpassed (18). The role of Ag dose in inducing T cells of different avidities and the impact of this on T cell-mediated pathogenesis therefore remain areas of uncertainty that are central to understanding the dynamics of T cell responses in vivo.

Despite characterization of the initial T cell response in peripheral lymphoid organs in mice immunized with encephalitogenic Ags, little is known about the sequelae that lead to overt disease (2, 17). This is in part due to the lack, until recently, of suitable approaches such as highly sensitive ELISPOT assays (17, 19) or appropriate peptide-MHC (pMHC) class II tetramers (20, 21) to assess the evolution of the autoreactive CD4$^+$ T cell response in quantitative terms. In the present study, we have used fluorescently labeled pMHC class II tetramers to enumerate autoantigen-specific

*Center for Immunology, [†]Department of Pathology, and [‡]Department of Molecular Biology, University of Texas Southwestern Medical Center, Dallas, TX 75390

Received for publication March 3, 2006. Accepted for publication October 10, 2006.

The costs of publication of this article were defrayed in part by the payment of page charges. This article must therefore be hereby marked *advertisement* in accordance with 18 U.S.C. Section 1734 solely to indicate this fact.

[1] This work was supported by grants from the National Institutes of Health (R01 AI/NS 42949), National Multiple Sclerosis Society (RG 2411), and Wadsworth Foundation. A.M. was supported by a Fellowship of the Fondo de Investigacion Sanitaria (BAE 00/5030 and 01/5037).

[2] A.M. and S.P. contributed equally to this study.

[3] Current address: Immunology Service, University Hospital "Virgen de la Arrixaca," El Palmar, Murcia, Spain.

[4] Current address: Ophthalmology Institute of Alicante (VISSUM), c/Cabanal, Alicante, Spain.

[5] Address correspondence and reprint requests to Dr. E. Sally Ward, Center for Immunology, University of Texas Southwestern Medical Center, 6000 Harry Hines Boulevard, Dallas, TX 75390-9093. E-mail address: sally.ward@utsouthwestern.edu

[6] Abbreviations used in this paper: EAE, experimental autoimmune encephalomyelitis; LN, lymph node; MBP, myelin basic protein; pMHC, peptide-MHC; tg, transgenic.

$CD4^+$ T cells in both peripheral lymphoid organs and the CNS following challenge of mice with different doses of MBP1-9 and the higher affinity position 4 analog, MBP1-9[4Y]. Relative to encephalitogenic Ag doses, a higher effective dose that is poorly encephalitogenic induces enhanced T cell responses that are accompanied by higher levels of cytokine (IFN-γ, TNF-α, and IL-17) production. Significantly, we show that a combination of anti-IFN-γ treatment with high effective Ag dose culminates in EAE. Thus, the challenge of mice with high Ag dose results in elevated levels of cytokine production that, in turn, down-regulate disease via a negative feedback loop. Our data have implications for understanding the factors that lead to pathogenesis in murine EAE, in addition to having broader relevance to the regulatory mechanisms that can occur to limit robust helper T cell responses that might otherwise be deleterious.

Materials and Methods

Peptides and Abs

The N-terminal peptide of myelin basic protein (MBP1-9, ASQKRPSQR, acetylated at residue 1) and (acetylated) analog MBP1-9 [4Y] with residue 4 (lysine) substituted by tyrosine were synthesized at the Peptide Synthesis Unit of the Howard Hughes Medical Institute, University of Texas Southwestern Medical Center, or CS Bio. Different batches of the peptides were used during the course of the experiments, and these induced similar behavior.

For flow cytometry studies the following fluorescently labeled Abs were purchased from BD Pharmingen: allophycocyanin-labeled anti-CD3 (145-2C11), Alexa 488-, FITC-, PerCP-, and allophycocyanin-labeled anti-CD4 (L3T4), anti-CD16/CD32 (Fc block, clone 2.4G2), PerCP-labeled anti-CD45 (30-F11), allophycocyanin-labeled anti-IFN-γ (XMG1.2), PE-labeled anti-TNF-α (MP6-XT22), PE-labeled anti-IL-17 (TC11-18H10), PE-labeled anti-TCR Vβ8 (F23.1), and FITC-labeled and purified anti-TCR Vα2 (B20.1). Purified anti-TCR Vα2 (BD Pharmingen) was labeled with Alexa 647 following the manufacturer's instructions (Molecular Probes). PE-labeled anti-F4/80 was purchased from eBioscience. Anti-I-A^u Ab was purified from the 10.2.16 hybridoma (22) and labeled with fluorescein-isothiocyanate using standard methods.

For use in vivo, hybridomas expressing anti-IFN-γ Ab (R4-6A2, rat IgG1 from the American Type Culture Collection) and rat IgG1 isotype control (CRL-1912 from the American Type Culture Collection) were grown up and IgG1 purified from culture supernatants using protein G-Sepharose. Hybridomas were grown in medium containing FCS that had been depleted of bovine IgGs by passage over protein G-Sepharose.

Generation of recombinant pMHC tetramers

Soluble, recombinant MBP1-9[4Y]:I-A^u complexes were generated and purified as described elsewhere (20). To detect MBP1-9-specific cells, multimeric complexes ("tetramers") were prepared by incubating site specifically biotinylated MBP1-9[4Y]:I-A^u with PE-labeled Extravidin (Sigma-Aldrich) in an optimized molar ratio for 10–30 min at 4°C (20).

Mice

B10. PL (H-2^u) mice were purchased from The Jackson Laboratory (Bar Harbor, ME). Transgenic (tg) mice expressing the 1934.4 TCR (12, 23) backcrossed onto the B10.PL background were provided by Dr. H. McDevitt (Stanford University, Stanford, CA) and were maintained by backcrossing onto B10. PL mice. Tg mice expressing the α- and β-chains of the 172.10 TCR (24, 25), backcrossed onto the B10.PL background, were provided by Dr. J. Goverman (University of Washington, Seattle, WA). These were interbred to generate tg mice expressing the 172.10 $\alpha\beta$ TCR. Mice were bred and maintained in the specific pathogen-free animal colony at the University of Texas Southwestern Medical Center in compliance with institutional guidelines. All mice were 7–10 wk of age when experiments were initiated. TCR tg animals selected as cell donors for transfer experiments did not show signs of spontaneous EAE (25) either before or at the time of the isolation.

Induction of EAE

For induction of EAE, B10.PL male mice were immunized s.c. in one footpad and the tail base with 200 μg of wild-type peptide MBP1-9, or with 2 or 200 μg of the higher affinity position 4 analog, MBP1-9[4Y] ("4Y") with the lysine at position 4 substituted by tyrosine (5–7). Peptide was emulsified in CFA (Sigma-Aldrich) supplemented with 4 mg/ml *Mycobacterium tuberculosis* H37RA (Difco; BD Biosciences), and the emulsion (100 μl/mouse) divided equally between the two immunization sites. As control, an emulsion of PBS and CFA was used. Pertussis toxin (List Biological Laboratories) (200 ng/mouse) in PBS was injected i.p. at the time of immunization and 48 h later. EAE scoring was performed as previously described (26): 0, no abnormality; 1, a limp tail; 2, moderate hind limb weakness; 3, severe hind limb weakness; 4, complete hind limb paralysis; 5, quadriplegia or premoribund state; and 6, death due to disease. Clinical signs of EAE were assessed for up to ~30 days after immunization. Mean clinical scores were derived from scores for all mice within each group and include disease-free mice. Mice that scored 4 for longer than 5 days or with a score of 5 were sacrificed, in accordance with institutional guidelines.

In transfer experiments, B10.PL mice were infused with splenocytes from tg mice expressing the 172.10 or 1934.4 TCRs (23, 25) before immunization. Numbers of $CD4^+$ splenocytes were determined by flow cytometry and different numbers of $CD4^+$ cells from tg mice were administered i.v. as a mix of total splenocytes through the tail vein. Pertussis toxin was not used when B10.PL animals were infused with splenocytes from tg mice. When required, splenocytes from tg mice were labeled with CFSE (Molecular Probes) as described previously (27).

Treatment of mice with anti-IFN-γ Ab

Mice immunized with 200 μg of MBP1-9[4Y] (as above) were treated with 30 or 100 μg of anti-IFN-γ Ab (rat IgG1, R4-6A2) by i.v. injection, on each of days 6 and 9 after immunization. One hundred micrograms of a rat IgG1 Ab of irrelevant specificity was also used for a different group of mice as a negative control. A group of B10.PL mice immunized with the encephalitogenic dose of 2 μg of MBP1-9[4Y] was also used as a control for disease induction. Immunized and treated mice were monitored daily from day 8 following immunization and disease severity scored.

Flow cytometric analyses

In experiments where CNS samples were analyzed, mice were anesthetized and perfused through the right ventricle with 10 ml of ice-cold PBS containing 2 mM $EDTANa_2$ before organ harvesting. Draining lymph nodes (LNs), spleens, and CNS tissue (brain and spinal cord) were harvested in RPMI 1640 containing 2 mM $EDTANa_2$ (Invitrogen Life Technologies) and single-cell suspensions obtained by forcing the tissue through a wire mesh tea strainer. RBC were lysed with ammonium chloride buffer and then cells washed with PBS. CNS homogenates were first centrifuged with a pulse of 1000 rpm to discard debris and then extensively washed in PBS.

For flow cytometric analyses, single-cell suspensions were incubated with Fc block for 5 min before incubation with appropriate combinations of Abs at 4°C in the presence of Fc block and then washed using standard methods. Ag (MBP1-9:I-A^u)-specific $CD4^+$ T cells in LNs, spleens, or CNS samples were quantitated by four-color flow cytometric analyses. Cells were incubated with PE-labeled MBP1-9[4Y]:I-A^u tetramer and fluorescently labeled Abs (as indicated in the figure legends) at 12°C for 2 h and washed twice before flow cytometric analyses. When anti-Vα2 (TCR) Ab was used, a two-step staining protocol was used. Following incubation with tetramer and other Abs at 12°C and one wash in PBS, cells were incubated with anti-Vα2 Ab at 4°C for 30 min and washed before analysis. Stained cells were analyzed using a FACSCalibur (BD Biosciences) and data analyzed using CellQuest (BD Biosciences) or WinMDI 2.8 (The Scripps Research Institute (http://facs.scripps.edu)).

To quantitate the absolute number of cells of each subpopulation in the samples, 50 μl of PBS containing 2×10^4 propidium iodide-labeled cells (BW5147 cells labeled by fixation and propidium iodide addition) was added to each tube immediately before flow cytometric analysis. The cell numbers in each subset were then calculated for each sample as described previously (28). Apoptotic/necrotic cells were assessed by staining with 5 μg/ml 7-aminoactinomycin D (BD Pharmingen).

Histological analyses

Brains and vertebral columns were harvested from mice between days 15 and 19 postimmunization by terminal cardiac perfusion with heparinized saline (10 U/ml) followed by 10% formalin. The brains were coronally sectioned, processed, and embedded in paraffin. Vertebral columns were decalcified in Cal-Rite (Richard-Allen Scientific) for 48 h, cut transversally into segments, and then processed and embedded in paraffin. Five-micrometer sections from each block were stained with H&E for microscopic examination.

The CNS sections of samples were scored for meningitis and myelitis in blinded fashion. For each mouse, two to three sections of brain and six to

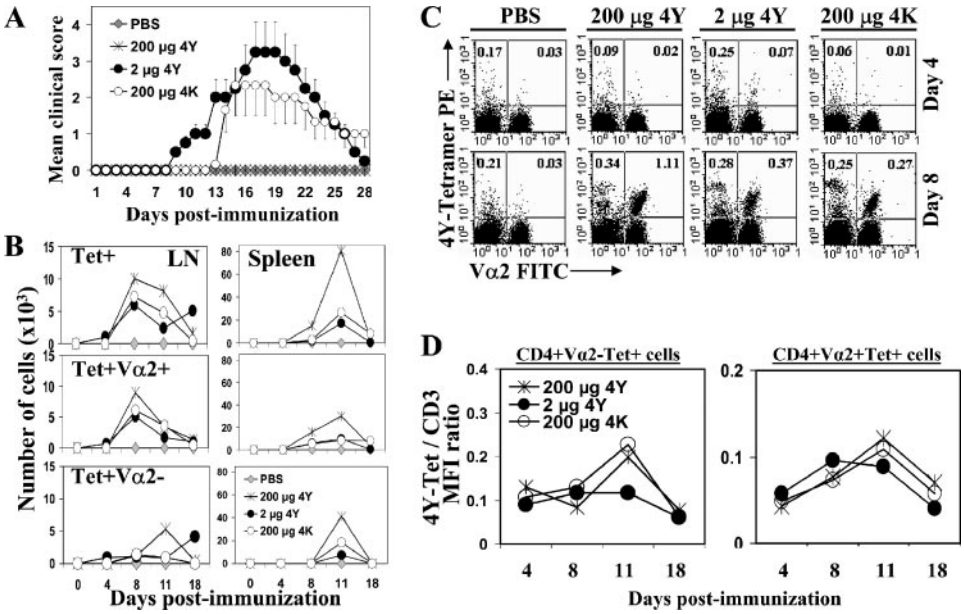

FIGURE 1. Induction of EAE and analysis of Ag-specific T cells in B10.PL mice following immunization with different doses of Ag. *A*, Mice (five per group) were immunized with PBS, 200 μg of MBP1-9 (4K), and 200 μg or 2 μg of MBP1-9[4Y] (4Y) peptide emulsified in CFA supplemented with 4 mg/ml mycobacterium. A total of 200 ng of pertussis toxin was administered i.p. on day 0 and day 2 postimmunization. The clinical score of EAE was determined daily as described in *Materials and Methods*. Disease incidence (numbers of mice showing disease symptoms/total number of mice) for each group was as follows: PBS, zero of five mice; 200 μg of 4K, four of six mice; 200 μg of 4Y, zero of five mice; and 2 μg of 4Y, five of five mice. Error bars, SEs. From days 16–24, significant differences (Mann-Whitney *U* test, $p < 0.05$) were seen between mice treated with 200 μg of 4Y and those treated with 2 μg of 4Y or 200 μg of 4K. *B*, Analyses of numbers of Ag-specific $CD4^+$ T cells using PE-labeled MBP1-9[4Y]:I-A^u tetramers (20). Numbers of $CD4^+$tetramer$^+$ (*top panels*), $CD4^+$tetramer$^+V\alpha2^+$ (*middle panels*), and $CD4^+$tetramer$^+V\alpha2^-$ (*bottom panels*) cells per mouse in spleens and pooled draining LNs in mice treated with different doses of Ag on the day of immunization (day 0) and days 4, 8, 11, and 18 postimmunization are shown. *C*, Dot plots showing the staining of Ag-specific T cells (with PE-labeled MBP1-9[4Y]:I-A^u tetramers; "4Y-tetramers") and FITC-labeled anti-Vα2 Ab in $CD4^+$ cells in LNs isolated from mice on days 4 and 8 postimmunization. Numbers on dot plots indicate the percentages of tetramer$^+V\alpha2^-$ and tetramer$^+V\alpha2^+$ cells within the $CD4^+$ populations. *D*, Plots of ratios of mean fluorescence intensity (MFI) for PE-labeled MBP1-9[4Y]:I-A^u tetramer ("4Y-tet") to MFI for allophycocyanin-labeled anti-CD3ε for both $CD4^+$tetramer$^+V\alpha2^-$ and $CD4^+$tetramer$^+V\alpha2^+$ populations from LNs analyzed directly ex vivo. Data in *B–D* show results from analyses of LNs or spleens pooled from two mice per group. All data are representative of at least two independent experiments.

eight sections across the entire length of spinal cord were examined microscopically. Quantitative analyses of inflammation were performed for spinal cord sections using Image J (http://rsb.info.nih.gov/ij/download.htm) to determine the circumference and area of each section. The scoring for meningitis was determined by calculating the number of inflammatory cell layers in the meninges and multiplying this number by the length of the meninges affected by inflammation (29). This length determination was subsequently divided by the circumference of the meninges and expressed as the percentage of the meninges with inflammation. Myelitis was evaluated by determining the area of each lesion. These areas were divided by the total area of each spinal cord section and expressed as the percentage of the spinal cord area showing myelitis (29). The histological score for each animal was derived from the average percentage of six to eight sections across the entire spinal cord.

In vitro stimulation assays

Spleen cells were cultured (6×10^6 cells/ml) in 96-well plates in complete DMEM containing 2 mM L-glutamine, 5×10^{-5} M 2-ME, 1 mM sodium pyruvate, 100 U/ml penicillin, 100 μg/ml streptomycin (Invitrogen Life Technologies), and 10% FCS for 96 h. MBP peptides were added at different concentrations (indicated in the figures). For the last 16 h of culture, 1 μCi of [^{3}H]thymidine (Amersham Biosciences) was added to each well. Proliferation is expressed as [^{3}H]thymidine incorporation (mean ± SE cpm of triplicate cultures). IFN-γ concentrations were determined in culture supernatants following 72 h of stimulation by ELISA as previously described (30) and expressed as mean ± SE of triplicate cultures.

Intracellular cytokine detection

Following immunization of B10.PL mice with different peptide doses, splenocytes were harvested and cultured (2×10^6 splenocytes/well) in 48-well plates in the presence of 50 μg/ml MBP1-9 or 10 μg/ml MBP1-9[4Y] in complete DMEM. For each condition, 4–6 wells were used. One microliter of the protein transport inhibitor GolgiPlug (BD Pharmingen), containing brefeldin A, was added per milliliter of medium. Cultures were maintained for 4 h at 37°C in a 5% CO_2 incubator. Cells were then harvested, washed twice with PBS, fixed with 5% formalin for 20 min at room temperature, washed once with PBS, once with 1% BSA/PBS, and permeabilized with 0.1% saponin in 1% BSA/PBS for 10 min at room temperature. Following fixation and permeabilization, cells were stained with FITC- or Alexa 488-labeled anti-CD4, allophycocyanin-labeled anti-IFN-γ and PE-labeled anti-IL-17, or allophycocyanin-labeled anti-CD4 and PE-labeled anti-TNF-α, washed, and analyzed by flow cytometry.

BrdU staining of cells in vivo

For BrdU staining, mice were injected twice (i.p.) 2 and 4 h before harvesting of LNs and splenocytes with 500 μg of BrdU (BD Pharmingen) per mouse. LN and spleen cells were isolated as above, washed twice with PBS, stained with PerCP-labeled anti-CD4, washed, fixed, permeabilized and treated with DNase for 60 min at 37°C to expose DNA labeled with BrdU. Cells were washed and stained with a FITC- (Caltag Laboratories) or allophycocyanin-labeled anti-BrdU Ab (BD Pharmingen) at room temperature for 20 min, washed and analyzed by flow cytometry as above.

Statistical analyses

For statistical analyses of disease incidence and in vitro T cell responses, Statistical Package for the Social software was used. Nonparametric tests appropriate to the sample size were applied. The Kruskal-Wallis test was used to compare all experimental groups, and when significant differences were found, the Mann-Whitney *U* test was used for pairwise comparisons. Histological data were analyzed using ANOVA. In all cases, *p* values of <0.05 were considered to indicate significant differences.

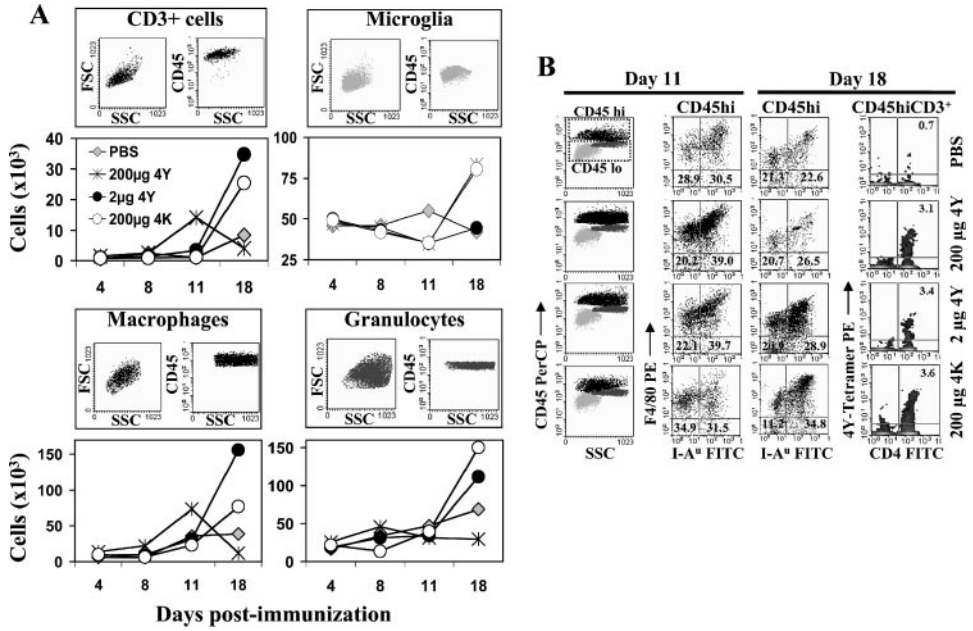

FIGURE 2. Analyses of CNS infiltrates following treatment of mice with different Ag doses. *A*, Determination of numbers of cells per mouse of the indicated subpopulations in mice following immunization with PBS, 200 μg of 4K and 2 μg or 200 μg of 4Y emulsified in CFA supplemented with 4 mg/ml mycobacterium. A total of 200 ng of pertussis toxin was administered i.p. on day 0 and day 2 postimmunization. Dot plots show forward scatter vs side scatter (FSC/SSC) and CD45 vs SSC for $CD3^+$ lymphocytes (black), microglia (light gray), macrophages (black), and granulocytes (dark gray). Data shown are derived from pooled CNS (brain and spinal cord) samples from two mice per group, sacrificed on days 4, 8, 11, and 18 postimmunization. *B*, Dot plots showing CNS infiltrates on days 11 and 18 postimmunization in mice treated as in *A*. The first column shows dot plots for staining with PerCP-labeled anti-CD45 vs SSC of the CNS samples. $CD45^{high}$ and $CD45^{low}$ windows were set in these plots (indicated by dotted lines), and dot plots for the $CD45^{high}$ populations stained with PE-labeled F4/80 vs FITC-labeled $I\text{-}A^u$ are shown for both days 11 and 18 postimmunization. Cell populations are indicated by colors as in *A*. Columns on the *right* of the figure show PE-labeled MBP1-9[4Y]:$I\text{-}A^u$ tetramer vs FITC-labeled CD4 staining for gated $CD45^{high}CD3^+$ cells on day 18 postimmunization. Numbers on dot plots indicate the percentages of cells in each population ($F4/80^{high}I\text{-}A^{u\ low}$ or $F4/80^{high}I\text{-}A^{u\ high}$ for $CD45^{high}$ cells, with numbers shown in *lower quadrants*, or $tetramer^+$ cells in the $CD45^{high}CD3^+$ populations). All data are representative of at least two independent experiments.

Results

Quantitative analyses of autoreactive T cells indicate a lack of correlation between EAE incidence and autoantigen specific T cell number

B10.PL ($H\text{-}2^u$) mice were immunized with the wild-type peptide MBP1-9 ("4K") (200 μg) with lysine at position 4, or the position 4 analog, MBP1-9[4Y] ("4Y") (2 or 200 μg) with lysine substituted by tyrosine. Due to the higher affinity of the 4Y analog for binding to $I\text{-}A^u$ (5–7), the use of this analog results in higher effective doses relative to 4K, even when the same total amount of peptide is used. The disease course in mice treated with different effective doses of peptide is shown in Fig. 1. Consistent with earlier reports (10), treatment of mice with 200 μg of 4Y results in either no EAE or a low incidence of mild disease (Fig. 1*A* and data not shown). Importantly, low doses (2 μg) of 4Y are as encephalitogenic as 200 μg of 4K (Fig. 1*A*), indicating that the difference in disease incidence following treatment with 200 μg of 4K vs 200 μg of 4Y is solely due to variations in effective peptide dose, rather than the position 4 substitution resulting in a conformational variant that does not elicit pathogenic T cells. In addition, the use of 2 μg of 4K did not induce disease (data not shown), indicating that this low-peptide dose falls below the threshold necessary to elicit EAE. This is also consistent with the data of others demonstrating that very low doses of 4Y (~20 ng) are not encephalitogenic (31).

Fluorescently labeled MBP1-9[4Y]:$I\text{-}A^u$ tetramers (20) were used to track and quantitate Ag-specific T cells at various times following immunization of B10.PL mice with different peptide doses. We also analyzed Vα2 expression by the Ag-specific T cells, because in B10.PL mice the TCR α-chain usage of encephalitogenic T cells is biased toward Vα2 usage with a lesser bias toward Vα4 (24). Clear populations of Ag-specific T cells could be detected in draining LNs and spleens 8 days following immunization (Fig. 1, *B* and *C*). This is followed by a peak of Ag-specific T cells in the spleen at day 11 (Fig. 1*B*). By day 18 postimmunization, the numbers of Ag-specific T cells in LNs and spleens have decreased to almost background levels (Fig. 1*B*). Significantly, the highest Ag dose (200 μg of 4Y) that is poorly encephalitogenic induces greater expansion of Ag-specific T cells relative to lower doses (200 μg of 4K or 2 μg of 4Y). This difference is particularly marked for splenocytes (Fig. 1*B*).

We also investigated the possibility that a high effective dose of Ag (200 μg of 4Y) results in the deletion of high-avidity cells from the peripheral repertoire (10), leaving a residual population of low-avidity cells that are not encephalitogenic. Such lower avidity cells might initially enter the CNS but be incapable of inducing an inflammatory infiltrate. The avidities of the Ag-specific T cells were investigated by analyzing the MBP1-9[4Y]:$I\text{-}A^u$ tetramer staining levels of T cells isolated from LNs of mice treated with different peptide doses (Fig. 1*D*). We have found that under the conditions of tetramer staining used, the fluorescence level is a reliable indicator of avidity of the T cells for pMHC ligand (32). For these experiments, TCR expression levels on cells were also analyzed and included as a normalization factor for tetramer staining levels (32, 33). This was necessary to ensure that differences in tetramer staining levels were not due to variations in extents of TCR downregulation. Although the availability of tetramer and LN cells limited these analyses to single data points per group, rather than dissociation analyses of tetramer staining (34), our observations

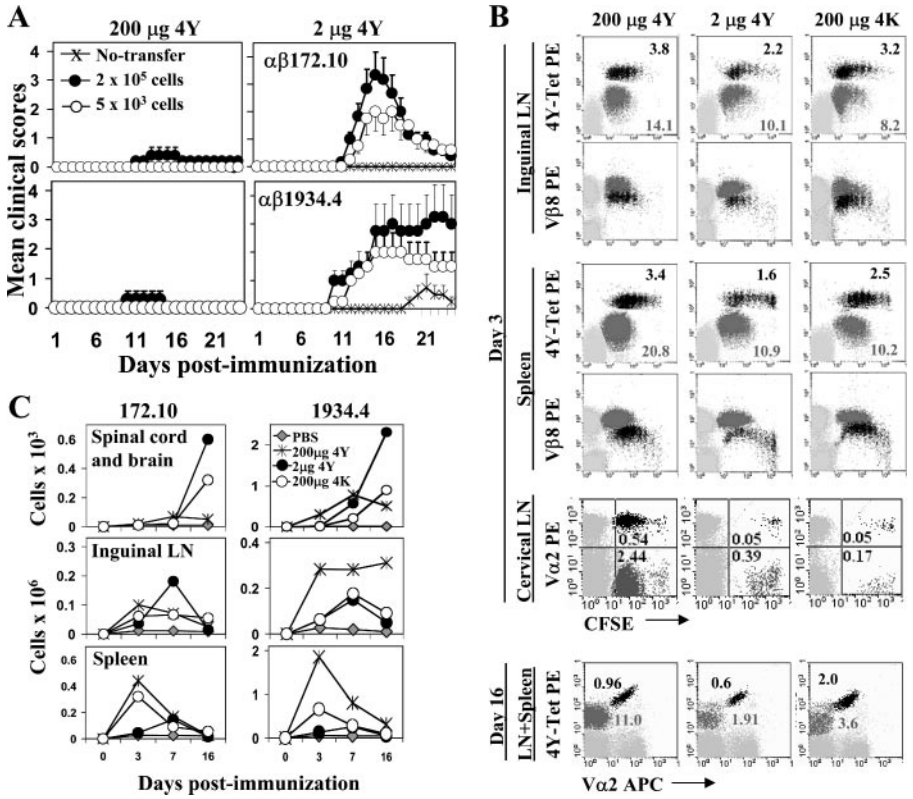

FIGURE 3. Analyses of behavior of transferred MBP1-9:I-A^u specific T cells bearing TCRs of known affinities for MBP1-9:I-A^u. *A*, EAE induction in B10.PL mice transferred with T cells derived from mice transgenically expressing either the 172.10 or 1934.4 TCR (23, 25). B10.PL males (five animals per group) were transferred with either 2×10^5, 5×10^3, or zero (no-transfer) CD4$^+$ cells mixed with splenocytes from 172.10 or 1934.4 tg mice and immunized with 200 or 2 μg of 4Y. Pertussis toxin was not used in these experiments. Clinical scores of EAE were determined daily as described in *Materials and Methods*. Disease incidence and mean disease scores for each group are shown in Table I. Error bars, SEs. From days 12–17 (172.10 tg T cells) and days 15–23 (1934.4 tg T cells) significant differences (Mann-Whitney *U* test, $p < 0.05$) were seen for mice transferred with 2×10^5 T cells and treated with 200 μg of 4Y or 2 μg of 4Y. There were no significant differences for mice transferred with 5×10^3 or 2×10^5 splenocytes followed by treatment with 2 μg of 4Y. *B*, Dot plots showing staining levels for CFSE- and PE-labeled MBP1-9[4Y]:I-A^u tetramer ("4Y-tet"), PE-labeled anti-TCR Vβ8 (F23.1), or PE labeled anti-Vα2 in LNs and spleens following immunization of mice transferred with 10^6 CFSE-labeled CD4$^+$ cells as a mixture of splenocytes from both 172.10 and 1934.4 tg mice and immunized as in *A*. 172.10 and 1934.4 tg T cells are indicated by black and dark gray dots, respectively. On day 3 postimmunization, CD4$^+$CFSE$^+$ 172.10 (Vα2$^+$) and CD4$^+$CFSE$^+$ 1934.4 (Vα2$^-$) tg cells were distinguished based on the levels of staining by tetramer (172.10 > 1934.4), anti-Vβ8 Ab (1934.4 > 172.10) or anti-Vα2 Ab, as indicated. By 4 days postimmunization, the CFSE signal was almost undetectable, and for day 16, postimmunization tg cells were therefore identified as CD4$^+$Tet$^+$Vα2$^+$ (primarily 172.10 tg T cells) and CD4$^+$Tet$^+$Vα2$^-$ (primarily 1934.4 tg T cells) as depicted in the *lowest panels*. Numbers on dot plots indicate the percentages of 172.10 or 1934.4 tg T cells within the CD4$^+$ populations (comprising both endogenous and tg CD4$^+$ cells). Data are derived from pooled samples from two mice per group. *C*, Numbers of 172.10 and 1934.4 tg T cells estimated as described in *B* in the CNS, inguinal LNs, and spleens at 0, 3, 7, and 16 days postimmunization. All data are representative of at least two independent experiments.

suggest that the avidities of the T cells between groups do not show marked differences when analyzed directly ex vivo (Fig. 1*D*).

The extent of infiltration of inflammatory cells correlates with EAE incidence and severity

As EAE is induced by T cell entry into the CNS followed by the infiltration of inflammatory cells (3, 35, 36), we next quantitated the numbers of infiltrating T cells, macrophages, and granulocytes in B10.PL mice following immunization with different effective doses of peptide (2, 200 μg of 4Y or 200 μg of 4K). The data in Fig. 2 show that, around the time of the peak of disease at day 18 postimmunization, encephalitogenic doses of peptide induce greater infiltration of T cells, macrophages, and granulocytes than a poorly encephalitogenic dose. Significantly, at a time point close to disease onset (day 11; Fig. 1*A*), infiltration of both T cells and macrophages can be observed in mice immunized with 200 μg of 4Y that are even slightly greater than those observed for encephalitogenic peptide doses (Fig. 2*A*). However, these infiltrates do not progress to the higher levels that are observed at day 18 in mice treated with encephalitogenic doses. Ag-specific T cells (assessed using pMHC tetramers) could also be detected at day 18 in the CNS in all groups of mice following Ag treatment. Although at day 18 postimmunization the numbers of infiltrating CD3$^+$ cells were much greater in mice treated with 200 μg of 4K or 2 μg of 4Y relative to those treated with 200 μg of 4Y, the percentages of Ag-specific cells among these cells were similar for all groups (Fig. 2*B*). At day 11, the percentages of Ag-specific T cells among the CD3$^+$ cells were 0.1, 1.3, 0.8, and 1.5% for mice treated with PBS, 200 μg of 4K, 2 μg of 4Y, and 200 μg of 4Y, respectively.

High-avidity T cells are not purged from the repertoire in response to immunization with high effective dose of Ag

To further investigate the behavior of Ag-specific T cells following the use of different effective peptide doses, we also analyzed B10.PL mice following adoptive transfer of different numbers of splenic T cells that transgenically express TCRs (172.10 and 1934.4) specific for MBP1-9:I-A^u (23, 25). Our earlier studies showed that the 172.10 and 1934.4 TCRs have affinities for pMHC

Table I. *EAE incidence in B10.PL male mice following transfer with 172.10 or 1934.4 tg cells and immunization with the indicated dose of Ag*

Type/No. Transferred Cells	Type of Immunization	n.s./n^a	Incidence (%)	Mortality (%)	Average EAE Score^b
No cell transfer	200 μg of 4Y	0/6	0	0	0
	2 μg of 4Y	0/6	0	0	0
172.10/5 $\times$ 10^3	PBS	0/3	0	0	0
	200 μg of 4Y	0/5	0	0	0
	2 μg of 4Y	2/4	50	0	2
172.10/2 $\times$ 10^5	PBS	0/3	0	0	0
	200 μg of 4Y	2/5	40	0	1.5
	2 μg of 4Y	6/6	100	0	3.25
1934.4/5 $\times$ 10^3	PBS	0/3	0	0	0
	200 μg of 4Y	0/4	0	0	0
	2 μg of 4Y	3/4	75	25	2.25
1934.4/2 $\times$ 10^5	PBS	0/3	0	0	0
	200 μg of 4Y	1/4	25	0	1
	2 μg of 4Y	3/4	75	50	3.25

[a] Number of animals with disease score $\geq$ 1.0 (sick animals)/total number of animals.
[b] Average of peak disease scores from animals with score $\geq$ 1.0.

ligand of 8.8 and 36.8 μM (32), respectively, and from tetramer staining analyses, their avidities fall at the high and low ends of the avidity spectrum of the Ag-specific repertoire in B10.PL mice (data not shown). Following transfer of these cells, mice were immunized with different peptide doses (2 or 200 μg of 4Y, in the absence of pertussis toxin) and disease incidence and severity analyzed (Fig. 3*A* and Table I). The data recapitulate the effects of using different Ag doses that are seen in B10.PL mice in the absence of T cell transfer but with pertussis toxin treatment (Fig. 1). Consistent with the known need for pertussis toxin for the effective induction of EAE, immunization of B10.PL mice without T cell transfer and pertussis toxin resulted in no disease or very mild disease at low incidence (Fig. 3*A* and Table I; no transfer).

We also analyzed the expansion of CFSE-labeled tg T cells in mice that were recipients of both high (172.10)- and low (1934.4)-avidity tg T cells. These mice were immunized with different effective doses of Ag and T cell expansion in spleens and LNs was analyzed 3 days later. 172.10 and 1934.4 tg T cells were distinguished based on the staining levels of tetramer (172.10 $>$ 1934.4) and TCR Vβ levels (172.10 $<$ 1934.4). The data show that both high- and low-avidity cells expand better in vivo in response to 200 μg of 4Y relative to 200 μg of 4K or 2 μg of 4Y (Fig. 3*B*). In addition, although 172.10 tg cells do not proliferate as well as 1934.4 cells, this is so for all Ag doses (and is also observed for in vitro proliferative responses of these tg cells; data not shown). Notably, even when the Ag dose differs by 100-fold (200 vs 2 μg of 4Y), the ratios of 172.10:1934.4 cells at 3 days following immunization are very similar (0.27 vs 0.22 for inguinal LNs, 0.16 vs 0.15 for splenocytes). This indicates that higher avidity cells are not preferentially expanded in the presence of low Ag dose and are also not preferentially deleted by high effective dose. Furthermore, at day 16 postimmunization both high (172.10; tetramer$^+$Vα2$^+$)- and low (1934.4; tetramer$^+$Vα2$^-$)-avidity cells could be readily detected in all groups of mice, although the CFSE staining levels were below the level of detection at this time (Fig. 3*B*, *lower panels*).

We also analyzed the expansion of transferred, CFSE-labeled tg T cells in the cervical LNs of mice treated with different effective doses of Ag (Fig. 3*B*). These LNs were chosen as they are both distal to the immunization site and drain the CNS. Given the difficulty in determining the concentration of functionally active peptide in vivo using, for example, labeled peptides, these analyses therefore give an indication of the distribution of Ag following the delivery of different doses. The data show substantially greater expansion of transferred tg cells of both high (172.10; Vα2$^+$)- and low (1934.4; Vα2$^-$)-avidity at day 3 posttransfer in mice immunized with 200 μg of 4Y relative to 2 μg of 4Y or 200 μg of 4K (Fig. 3*B*). These observations support the idea that the high concentration of peptide diffuses and persists throughout the body where it can effectively restimulate Ag-specific cells.

The higher numbers of Ag-specific T cells in the transfer experiments also facilitated their quantitation in the CNS. The numbers and pattern of infiltrating, tetramer-positive cells show a very similar trend to that observed for CD3$^+$ cells in B10.PL mice without cell transfer (Figs. 2*A* and 3*C*). Before disease onset, Ag-specific cells in the CNS are greater in number in 200 μg of 4Y-treated mice relative to those in mice immunized with 200 μg of 4K or 2 μg of 4Y, but at the peak of disease, this is clearly reversed. Furthermore, in both draining LNs and spleens, the Ag-specific cells are in general present in higher numbers following treatment with 200 μg of 4Y, with the differences being most marked at day 3 postimmunization (Fig. 3, *B* and *C*). Although we cannot exclude the contribution of endogenous Ag-specific cells to the total cell numbers determined in these experiments, the numbers of Ag-specific cells in immunized B10.PL mice are ~100-fold lower in mice that were not recipients of transferred cells (Figs. 1*B* and 3*C*). Analyses of the percentages of apoptotic/necrotic cells in recipients of CFSE-labeled tg cells showed slightly higher percentages for mice immunized with 2 μg of 4Y relative to 200 μg of 4Y at day 3 postimmunization that were more marked in the CFSE-negative CD4$^+$ (endogenous) cells (data not shown). The data indicate that relative to 200 μg of 4K or 2 μg of 4Y, 200 μg of 4Y induces greater expansion of both high- and low-avidity cells, and these differences become very marked at sites such as the cervical LNs that are distal to the immunization site. Taken together with the data presented in Fig. 2, there appears to be little evidence for the deletion of high-avidity cells following immunization with 200 μg of 4Y.

A high effective dose of Ag does not result in T cell hyporesponsiveness

Although the data in Fig. 1 suggest that the responding T cells from mice treated with different peptide doses do not appear to differ in avidity for cognate pMHC ligand, it is still possible that they differ in "functional avidity" (37). To investigate this possibility, proliferation and cytokine production by Ag-specific T cells

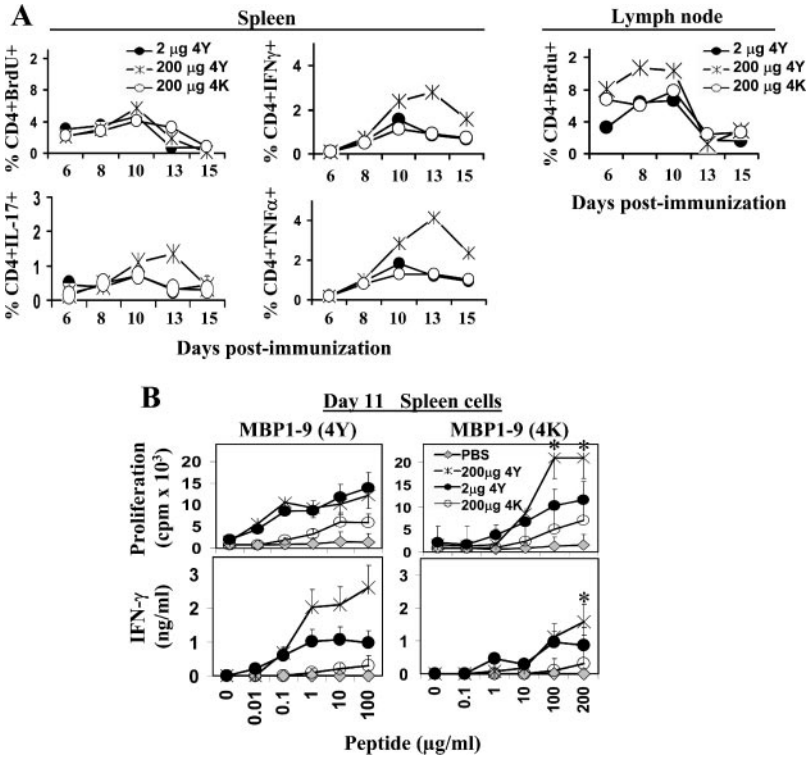

FIGURE 4. T cell responses following immunization of mice with different Ag doses. *A*, B10.PL mice were immunized with 200 μg of 4K and 2 μg or 200 μg of 4Y peptide emulsified in CFA supplemented with 4 mg/ml mycobacterium. A total of 200 ng of pertussis toxin was administered i.p. on day 0 and day 2 postimmunization. LNs and spleens were isolated from mice (pooled from two mice per group per time point) at days 6, 8, 10, 13, and 15 postimmunization. Two and 4 h before harvesting LNs and spleens, mice were injected with BrdU. Numbers of $CD4^+BrdU^+$ cells were determined by flow cytometry. Splenocytes were incubated with 10 μg/ml 4Y for 4 h in the presence of GolgiPlug, and then $CD4^+IL\text{-}17^+$, $CD4^+IFN\text{-}\gamma^+$, and $CD4^+TNF\text{-}\alpha^+$ cells quantitated by intracellular staining and flow cytometry. *B*, Proliferation and IFN-γ secretion of splenocytes isolated from mice (pooled from two to three mice per group) following in vitro restimulation. Splenocytes were harvested from mice on day 11 following immunization with different peptide doses (as for *A*; symbols used for different peptide doses or PBS are shown in the *inset* in the *upper right panel*). The peptide (4K or 4Y) used for in vitro recall is indicated above the panels. Error bars indicate SEs. *, $p < 0.05$ (Mann-Whitney *U* test), comparing cells from mice immunized with 200 μg of 4Y vs cells from mice immunized with 2 μg of 4Y, 200 μg of 4K, or PBS (control). All data are representative of at least three independent experiments.

were quantitated by BrdU uptake and intracellular cytokine staining of ex vivo T cells isolated from the LNs and spleens of mice treated with different doses of peptide. On days 8 and 10 following immunization, the LN cells from 200 μg of 4Y-treated mice were proliferating more than those from mice treated with encephalitogenic peptide doses (Fig. 4*A*). This is consistent with the increased number of Ag-specific T cells (Fig. 1). Splenocytes from mice immunized with 200 μg of 4Y also produced more IFN-γ and TNF-α following in vitro restimulation for 4 h, with the difference becoming most marked on day 13 (Fig. 4*A*). Recently, IFN-γ has been shown to inhibit the development of IL-17-producing $CD4^+$ T cells (Th-17 cells) that are associated with autoimmunity (38–41). We therefore analyzed IL-17 production in the different groups of mice. Importantly, IL-17-producing cells were also more abundant in mice treated with a high effective dose of Ag, indicating that the inhibition of development of this lineage of cells is not related to the low disease incidence following immunization with 200 μg of 4Y. In addition, we could not detect IL-4 or IL-10 in the cultures at any stage postimmunization (data not shown).

We also analyzed the proliferative and IFN-γ responses of splenocytes isolated from mice in the different groups at 11 days postimmunization followed by in vitro stimulation for 3–4 days (Fig. 4*B*). We observed that consistent with the ex vivo analyses (Fig. 4*A*), cells isolated from mice treated with the highest effective peptide dose (200 μg of 4Y) generally showed the greatest proliferative and cytokine (IFN-γ) responses, indicating that this

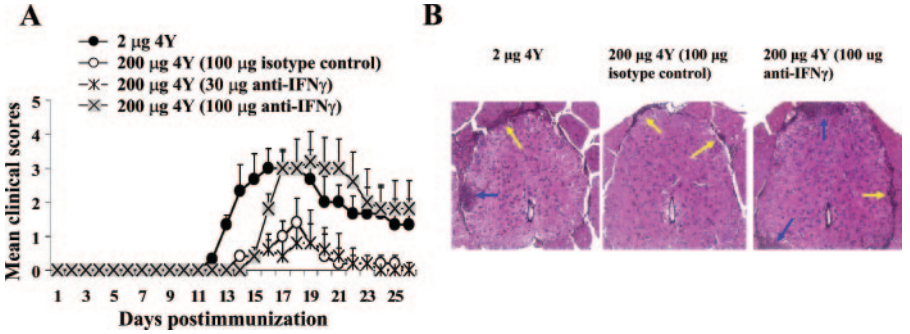

FIGURE 5. Anti-IFN-γ Ab treatment in combination with 200 μg of 4Y induces severe EAE. *A*, B10.PL mice were immunized with 200 μg of 4Y peptide emulsified in CFA supplemented with 4 mg/ml mycobacterium. A total of 200 ng of pertussis toxin was administered i.p. on day 0 and day 2 postimmunization. Mice (five per group) were injected i.v. with 30 or 100 μg of anti-IFN-γ Ab or 100 μg of isotype-matched control Ab on days 6 and 9 postimmunization. As a control for disease induction, mice were also immunized with 2 μg of 4Y followed by pertussis toxin as above. Disease incidence (numbers of mice showing disease symptoms/total number of mice) for each group was as follows: 2 μg of 4Y, three of three mice; 200 μg of 4Y plus 100 μg of anti-IFN-γ Ab, four of five mice; 200 μg of 4Y plus 30 μg of anti-IFN-γ Ab, two of five mice; 200 μg of 4Y plus 100 μg of isotype-matched control Ab, two of five mice. Error bars, SEs. For days 14–26, differences between mice treated with 2 μg of 4Y or 200 μg of 4Y plus 100 μg of anti-IFN-γ Ab were not significant, whereas there were significant differences between mice treated with 2 μg of 4Y or 200 μg of 4Y plus isotype control (Mann-Whitney *U* test, $p < 0.05$; from data pooled from three independent experiments). *B*, Mice (four per group) were treated as in *A*, except that there was no group treated with 200 μg of 4Y plus 30 μg of anti-IFN-γ Ab. Representative H&E-stained sections of spinal cord show inflammatory lesions. The lesions included both meningitis (indicated by yellow arrows) and myelitis (indicated by blue arrows).

Table II. *Histological analyses in mice treated with Ag plus anti-IFN-γ Ab*

Treatment[a]	Meningitis[b]	Myelitis[b]
2 μg of 4Y	1.67 ± 0.69	0.28 ± 0.19
200 μg of 4Y plus 100 μg of isotype control	0.18 ± 0.14	0.00 ± 0.01
200 μg of 4Y plus 100 μg of anti-IFN-γ	1.65 ± 1.12[c]	0.39 ± 0.28[c]

[a] Mice were treated as in Fig. 5*B*.

[b] Sizes of inflammatory lesions were assessed as in Ref. 29 and *Materials and Methods*, and mean values for all sections within each treatment group are shown. For each mouse (four mice per group), six to eight sections of spinal cord were analyzed.

[c] Indicates significantly different compared with values for mice treated with 200 μg of 4Y followed by isotype-matched Ab (ANOVA, $p = 0.032$ for myelitis, $p = 0.04$ for meningitis), and not significantly different compared with mice treated with 2 μg of 4Y (ANOVA, $p = 0.54$ for myelitis, $p = 0.98$ for meningitis).

poorly encephalitogenic dose of Ag does not generate $CD4^+$ cells that are refractory to restimulation. Thus, the inability of T cells from mice immunized with 200 μg of 4Y to induce disease does not appear to be due to lower cytokine production nor to an inability of the cells to proliferate in response to Ag. Indeed, upon restimulation, these cells consistently produce higher levels of IFN-γ relative to $CD4^+$ T cells from mice immunized with lower effective doses. Taken together with the indication from the cervical LN analyses that immunization with a high effective dose of peptide results in a broad distribution of Ag (Fig. 3*B* and data not shown), the data in Fig. 4 suggest that high nonencephalitogenic doses of 4Y peptide result in increased levels of IFN-γ at diffuse sites in the body.

The combination of anti-IFN-γ Ab treatment and high effective dose of Ag induces severe EAE

Our data suggest that the high levels of IFN-γ that are produced by Ag-specific T cells following treatment of mice with 200 μg of 4Y might be related to the low disease incidence. However, this does not causally link elevated IFN-γ levels to resistance to EAE. We therefore investigated whether lowering IFN-γ levels in the presence of treatment with 200 μg of 4Y would result in overt autoimmunity. Mice were immunized and treated with different doses of anti-IFN-γ (Fig. 5*A*). Immunization with 200 μg of 4Y followed by i.v. delivery of 100 μg of anti-IFN-γ Ab on each of days 6 and 9 results in disease incidence and severity similar to that induced by 2 μg of 4Y, although the disease shows a slightly later onset. The use of lower doses of anti-IFN-γ Ab (30 μg) does not have any effect. The elevated levels of IFN-γ that result from treatment with 200 μg of 4Y are therefore protective against EAE.

Histological analyses of mice treated as in Fig. 5*A* were also conducted. Lesions in all groups of mice consisted of a mild-to-moderate, focal, nonsuppurative meningitis, and myelitis in the lumbar and cervical segments of spinal cords and minimal meningitis in the pons and cerebrum, with higher numbers of lesions in mice treated with 200 μg of 4Y plus anti-IFN-γ Ab relative to mice treated with 200 μg of 4Y plus isotype-matched control Ab (Fig. 5*B* and data not shown). Quantitative analyses of the meningitis and myelitis indicated no significant differences between mice treated with 2 μg of 4Y and 200 μg of 4Y plus anti-IFN-γ Ab, whereas significant differences were seen between these two groups and mice treated with 200 μg of 4Y plus isotype-matched Ab (Table II).

Discussion

Despite relevance to multiple aspects of T cell biology, there is a paucity of knowledge concerning possible correlations between (auto)antigen dose and the characteristics of the responding T cells. In the current study, we have analyzed the dynamic properties of the immune response in H-2^u mice following immunization with different doses of the N-terminal epitope of MBP (MBP1-9) or its higher affinity position 4 analog, MBP1-9[4Y], that binds to I-A^u with 10^3- to 10^4-fold higher affinity (7, 10). Significantly, we show an inverse correlation between the strength of Ag-specific T cell responses, including IFN-γ production, and disease activity. Furthermore, the pMHC tetramer staining levels of the Ag-specific T cells are not altered by Ag dose such that higher avidity cells would correlate with disease incidence and severity. Taken together with our observation that a poorly encephalitogenic high dose of Ag can be converted into an efficient inducer of disease in the presence of anti-IFN-γ Ab, our results indicate that the inability of high effective doses of Ag to elicit EAE is causally related to a negative feedback loop in which this cytokine is centrally involved.

We show that a poorly encephalitogenic high dose of Ag induces a robust peripheral T cell response that results in enhanced levels of IFN-γ, TNF-α, and IL-17 relative to those seen in mice treated with lower Ag doses that progress to severe EAE. Following immunization with high or low effective doses of Ag, T cells enter the CNS between days 8 and 11 postimmunization. Significantly, higher numbers of infiltrating T cells, macrophages, and granulocytes are observed at a time point (day 11) immediately before the expected time of disease onset in mice treated with a poorly encephalitogenic high dose of Ag relative to mice immunized with lower doses. Ag-specific T cells, enumerated using pMHC tetramers, comprise a low percentage of the infiltrating $CD4^+$ cells for all doses of Ag. Similarly, in MBP79-89-induced EAE in SJL mice, Ag-specific T cells assessed by ELISPOT assays represented a low proportion (1 in 300) of total $CD4^+$ cells in the CNS (17), in contrast to studies in which the entry of passively transferred T cells were quantitated (42). Remarkably, the CNS infiltrates in mice treated with high dose of Ag, although initially greater in magnitude than those treated with lower encephalitogenic doses, do not progress to higher levels. Rather, they show a decrease, while substantial increases in infiltration of inflammatory cells are observed in mice that succumb to disease following immunization with lower doses of Ag.

The question therefore arises as to why, following immunization with a high dose (200 μg) of MBP1-9[4Y], the initial CNS infiltrate does not progress further to culminate in disease? Restimulation of infiltrating T cells in the CNS has been shown to be involved in the pathogenesis of EAE (43, 44). One possibility is that a high Ag dose results in alteration of the peripheral repertoire to induce T cells of low (functional) avidity that, following entry into the CNS, cannot be restimulated to induce an inflammatory infiltrate (10). However, our data would argue against this. First, a high effective dose of Ag results in T cells that produce greater levels of cytokines (IFN-γ, IL-17, and TNF-α) and proliferate more both in vivo and in vitro compared with T cells in mice treated with encephalitogenic doses. Second, at around day 11, we observe greater numbers of inflammatory cells in the CNS of mice treated with a high effective dose of Ag relative to those that will succumb to disease, suggesting that the initial infiltrate is prorather than anti-inflammatory. Our results suggest that following entry into the CNS, a regulatory mechanism prevails in mice that are treated with high dose of Ag that arrests further inflammation and the manifestation of disease. Furthermore and consistent with the conclusions drawn from ELISPOT analyses by Lehmann and colleagues (17) in a distinct model of EAE, these observations indicate that the analysis of peripheral T cell numbers and properties may not be a useful predictor of disease in EAE.

Importantly, the combination of high Ag dose (200 μg of 4Y) and anti-IFN-γ treatment results in the onset of severe disease. Taken together with the greater responsiveness of Ag-specific T cells following high dose Ag treatment, our data are therefore consistent with a model in which low levels of IFN-γ are proinflammatory, but once a certain threshold of stimulation and concentration of IFN-γ is reached, the anti-inflammatory role of IFN-γ becomes dominant. This threshold might also be reached in, for example, Drak2$^{-/-}$ mice (45) that in contrast to other models of T cell hyperresponsiveness (30) are resistant to EAE induction. An anti-inflammatory role for IFN-γ in EAE is well documented. For example, genetic deletion of either the IFN-γ or IFN-γ receptor gene leads to exacerbation of EAE in mice (46–48). In addition, anti-IFN-γ treatment can worsen disease (3, 49, 50) whereas intrathecal IFN-γ delivery or high IFN-γ levels induced by early IL-12 administration can protect against EAE (51, 52). High doses of (auto)antigen, as used in the current study, might therefore induce a regulatory feedback mechanism that through IFN-γ effects serves to down-regulate robust T cell responses that might otherwise be damaging. Consistent with this concept, using in vivo proliferative responses of autoreactive T cells as a readout, we show that a poorly encephalitogenic high dose of Ag results in more potent T cell stimulation in LNs, including the cervical LNs, and spleens relative to lower encephalitogenic doses.

Data to support various mechanisms for the anti-inflammatory effects of IFN-γ have been described, and these include antiproliferative and proapoptotic effects that involve NO production by macrophages or resident microglia (53–57) or the inhibition of the development of IL-17-producing CD4$^+$ cells that are associated with autoimmunity (38–41). Our immunohistological analyses indicate no major differences in the numbers of apoptotic cells in the mice in the different groups (data not shown), but this may be due to the greater number of infiltrating cells at the peak of disease in the lower Ag dose groups combined with the susceptibility of infiltrating CD4$^+$ cells to undergo apoptosis in the CNS (58–60). IFN-γ has also been shown to result in hyporesponsiveness in T cells by inducing CD3ζ down-regulation (61), but we do not observe differences in intracellular CD3ζ levels (data not shown) nor T cell hyporesponsiveness in mice treated with higher doses of Ag. Furthermore, we observe greater numbers of IL-17-producing CD4$^+$ cells following treatment of mice with a high effective dose of Ag, indicating that in the current study the protective effects of IFN-γ are not through the inhibition of the development of Th-17 (IL-17 producing) cells.

Recent studies have shown that Gr1$^+$ myeloid cells that are dependent on IFN-γ production by CD4$^+$ T cells can play a role in regulating EAE (62). We observe Gr1$^+$ cells in the CNS of mice treated with both high and low effective doses of Ag (data not shown). Thus, during the early stages of infiltration, higher levels of IFN-γ produced either systemically or locally by infiltrating CD4$^+$ cells in the CNS in response to relatively high levels of (exogenous) Ag might provide an environment that is conducive to the induction of the regulatory activity of Gr1$^+$ cells. The diffuse, and functionally active, peptide distribution following the delivery of high doses of MBP1-9[4Y] would be predicted to support local stimulation and IFN-γ secretion in the CNS. Infiltrating Gr1$^+$ cells could then, via NO mediated pathways (62–64), down-regulate the inflammatory process and halt the sequelae that lead to overt disease.

Our observations do not exclude the additional involvement of TNF-α in down-modulating disease. In this context, greater levels of TNF-α are produced following the use of a high effective dose of Ag relative to lower doses, in a pattern that resembles that of IFN-γ production. TNF-α has been shown in multiple models to have anti-inflammatory effects via mechanisms that include apoptosis induction, IL-12/IL-23 inhibition, or CD3ζ down-regulation (65–69). However, we clearly show that reduction of elevated IFN-γ levels is sufficient to reverse the protective effects of treatment with a high dose of Ag, placing IFN-γ as a central regulator of the disease process.

The experiments in this study demonstrate that when analyzed directly ex vivo, the Ag dose does not affect the avidities of the responding T cells in a way that would explain the differences in disease incidence. These data would appear to be discordant with earlier studies in which Ag-specific T cells derived from H-2^u mice immunized with MBP1-9 or position 4 analogs (4A and 4Y) were analyzed and deletion of high-avidity peripheral T cells by higher doses of Ag was reported (10). However, the T cell lines and hybridomas analyzed in the earlier study had been restimulated in vitro with varying Ag doses. The possibility that changes in the responding T cell repertoire had occurred during restimulation can therefore not be excluded. Such alteration of the avidities of T cells during in vitro cultivation has been observed by others in distinct Ag recognition systems (70, 71). The effect of varying Ag dose in the current study therefore appears to impinge on the robustness of the primary response but does not affect the qualitative nature of the responding repertoire in terms of T cell avidity. Such observations are consistent with those of McHeyzer-Williams and colleagues (18) where primary T cell responses to cytochrome *c* were studied, and, above a certain threshold, no major differences in repertoire were observed over a wide range of Ag doses. Consistent with the current study, ELISPOT assays of CD4$^+$ T cells in the MBP79-89/SJL mouse model of EAE provided little evidence for the preferential recruitment and expansion of high-avidity cells in the CNS, suggesting that selection for such cells does not play a role in pathogenesis (17). Our data concerning the adoptive transfer of T cells from tg mice expressing the 1934.4 and 172.10 TCRs that have different affinities for Ag (32) are in accord with the concept that above a certain avidity threshold, cells of both high and low avidity can be involved in disease progression. However, this does not exclude a role for high-avidity "driver" clones such as T cells bearing the 172.10 TCR (with CDR3β "DAGGGY" motif) in the development of EAE (72–74).

Our studies have implications for understanding the factors that lead to overt autoimmunity, with a particular focus on the nature of the autoreactive T cell response. They indicate that high doses of Ag induce a regulatory feedback mechanism that limits the response through IFN-γ-mediated effects. This has direct relevance to the treatment of autoimmunity by targeting cytokines such as IFN-γ that can have both pro- and anti-inflammatory effects. We also show that autoreactive T cell number and production of cytokines such as IFN-γ, TNF-α, and IL-17 in the periphery are not useful predictors of progression to overt disease. These analyses have broader relevance that extend beyond understanding autoimmunity to, for example, the development of vaccines for which a robust Th1-type response is required. Specifically, to protect against potential damage caused by inflammation, responses above a given threshold may be susceptible to the regulatory effects of IFN-γ and therefore less efficacious than milder immunization regimes.

Acknowledgments

We thank James Johnson, Fernando Mateos, Carlos Vaccaro, Sylvia Wanjie, and Steven Gibbons for expert technical assistance. John Shelton and Guadalupe Ruiz Merino provided expert assistance with histological and statistical analyses, respectively. We are also indebted to Drs. Hugh McDevitt and Joan Goverman for providing the tg mice used in this study.

Disclosures

The authors have no financial conflict of interest.

References

1. Brown, A., D. E. McFarlin, and C. S. Raine. 1982. Chronologic neuropathology of relapsing experimental allergic encephalomyelitis in the mouse. *Lab. Invest.* 46: 171–185.
2. Steinman, L., R. Martin, C. Bernard, P. Conlon, and J. R. Oksenberg. 2002. Multiple sclerosis: deeper understanding of its pathogenesis reveals new targets for therapy. *Annu. Rev. Neurosci.* 25: 491–505.
3. Elhofy, A., K. J. Kennedy, B. T. Fife, and W. J. Karpus. 2002. Regulation of experimental autoimmune encephalomyelitis by chemokines and chemokine receptors. *Immunol. Res.* 25: 167–175.
4. Zamvil, S. S., D. J. Mitchell, A. C. Moore, K. Kitamura, L. Steinman, and J. B. Rothbard. 1986. T cell epitope of the autoantigen myelin basic protein that induces encephalomyelitis. *Nature* 324: 258–260.
5. Fairchild, P. J., R. Wildgoose, E. Atherton, S. Webb, and D. C. Wraith. 1993. An autoantigenic T cell epitope forms unstable complexes with class II MHC: a novel route for escape from tolerance induction. *Int. Immunol.* 5: 1151–1158.
6. Mason, K., D. W. J. Denney, and H. M. McConnell. 1995. Myelin basic protein peptide complexes with the class II MHC molecules I-A^u and I-A^k form and dissociate rapidly at neutral pH. *J. Immunol.* 154: 5216–5227.
7. Fugger, L., J. Liang, A. Gautam, J. B. Rothbard, and H. O. McDevitt. 1996. Quantitative analysis of peptides from myelin basic protein binding to the MHC class II protein, I-A^u, which confers susceptibility to experimental allergic encephalomyelitis. *Mol. Med.* 2: 181–188.
8. Liu, G. Y., P. J. Fairchild, R. M. Smith, J. R. Prowle, D. Kioussis, and D. C. Wraith. 1995. Low avidity recognition of self-antigen by T cells permits escape from central tolerance. *Immunity* 3: 407–415.
9. Harrington, C. J., A. Paez, T. Hunkapiller, V. Mannikko, T. Brabb, M. Ahearn, C. Beeson, and J. Goverman. 1998. Differential tolerance is induced in T cells recognizing distinct epitopes of myelin basic protein. *Immunity* 8: 571–580.
10. Anderton, S. M., C. G. Radu, P. A. Lowrey, E. S. Ward, and D. C. Wraith. 2001. Negative selection during the peripheral immune response to antigen. *J. Exp. Med.* 193: 1–11.
11. He, X., C. Radu, J. Sidney, A. Sette, E. S. Ward, and K. C. Garcia. 2002. Structural snapshot of aberrant antigen presentation linked to autoimmunity: the immunodominant epitope of MBP complexed with I-A^u. *Immunity* 17: 83–94.
12. Wraith, D. C., D. E. Smilek, D. J. Mitchell, L. Steinman, and H. O. McDevitt. 1989. Antigen recognition in autoimmune encephalomyelitis and the potential for peptide-mediated immunotherapy. *Cell* 59: 247–255.
13. Amrani, A., J. Verdaguer, P. Serra, S. Tafuro, R. Tan, and P. Santamaria. 2000. Progression of autoimmune diabetes driven by avidity maturation of a T cell population. *Nature* 406: 739–742.
14. Gronski, M. A., J. M. Boulter, D. Moskophidis, L. T. Nguyen, K. Holmberg, A. R. Elford, E. K. Deenick, H. O. Kim, J. M. Penninger, B. Odermatt, et al. 2004. TCR affinity and negative regulation limit autoimmunity. *Nat. Med.* 10: 1234–1239.
15. Han, B., P. Serra, J. Yamanouchi, A. Amrani, J. F. Elliott, P. Dickie, T. P. DiLorenzo, and P. Santamaria. 2005. Developmental control of CD8 T cell-avidity maturation in autoimmune diabetes. *J. Clin. Invest.* 115: 1879–1887.
16. McCue, D., K. R. Ryan, D. C. Wraith, and S. M. Anderton. 2004. Activation thresholds determine susceptibility to peptide-induced tolerance in a heterogeneous myelin-reactive T cell repertoire. *J. Neuroimmunol.* 156: 96–106.
17. Hofstetter, H. H., O. S. Targoni, A. Y. Karulin, T. G. Forsthuber, M. Tary-Lehmann, and P. V. Lehmann. 2005. Does the frequency and avidity spectrum of the neuroantigen-specific T cells in the blood mirror the autoimmune process in the central nervous system of mice undergoing experimental allergic encephalomyelitis? *J. Immunol.* 174: 4598–4605.
18. Malherbe, L., C. Hausl, L. Teyton, and M. G. McHeyzer-Williams. 2004. Clonal selection of helper T cells is determined by an affinity threshold with no further skewing of TCR binding properties. *Immunity* 21: 669–679.
19. Targoni, O. S., J. Baus, H. H. Hofstetter, M. D. Hesse, A. Y. Karulin, B. O. Boehm, T. G. Forsthuber, and P. V. Lehmann. 2001. Frequencies of neuroantigen-specific T cells in the central nervous system versus the immune periphery during the course of experimental allergic encephalomyelitis. *J. Immunol.* 166: 4757–4764.
20. Radu, C. G., S. M. Anderton, M. Firan, D. C. Wraith, and E. S. Ward. 2000. Detection of autoreactive T cells in H-2^u mice using peptide-MHC multimers. *Int. Immunol.* 12: 1553–1560.
21. Reddy, J., E. Bettelli, L. Nicholson, H. Waldner, M. H. Jang, K. W. Wucherpfennig, and V. K. Kuchroo. 2003. Detection of autoreactive myelin proteolipid protein 139–151-specific T cells by using MHC II (IAs) tetramers. *J. Immunol.* 170: 870–877.
22. Oi, V. T., P. P. Jones, J. W. Goding, and L. A. Herzenberg. 1978. Properties of monoclonal antibodies to mouse Ig allotypes, H-2, and Ia antigens. *Curr. Top. Microbiol. Immunol.* 81: 115–120.
23. Pearson, C. I., W. van Ewijk, and H. O. McDevitt. 1997. Induction of apoptosis and T helper 2 (Th2) responses correlates with peptide affinity for the major histocompatibility complex in self-reactive T cell receptor transgenic mice. *J. Exp. Med.* 185: 583–599.
24. Urban, J. L., V. Kumar, D. H. Kono, C. Gomez, S. J. Horvath, J. Clayton, D. G. Ando, E. E. Sercarz, and L. Hood. 1988. Restricted use of T cell receptor V genes in murine autoimmune encephalomyelitis raises possibilities for antibody therapy. *Cell* 54: 577–592.
25. Goverman, J., A. Woods, L. Larson, L. P. Weiner, L. Hood, and D. M. Zaller. 1993. Transgenic mice that express a myelin basic protein-specific T cell receptor develop spontaneous autoimmunity. *Cell* 72: 551–560.
26. Critchfield, J. M., M. K. Racke, J. C. Zuniga-Pflucker, B. Cannella, C. S. Raine, J. Goverman, and M. J. Lenardo. 1994. T cell deletion in high antigen dose therapy of autoimmune encephalomyelitis. *Science* 263: 1139–1143.
27. Lyons, A. B., and C. R. Parish. 1994. Determination of lymphocyte division by flow cytometry. *J. Immunol. Methods* 171: 131–137.
28. Marin, L., A. Minguela, A. Torio, M. R. Moya-Quiles, M. Muro, O. Montes-Ares, A. Parrado, D. M. Alvarez-Lopez, and A. M. Garcia-Alonso. 2003. Flow cytometric quantification of apoptosis and proliferation in mixed lymphocyte culture. *Cytometry A* 51: 107–118.
29. Mi, W., M. Belyavskyi, R. R. Johnson, A. N. Sieve, R. Storts, M. W. Meagher, and C. J. Welsh. 2004. Alterations in chemokine expression following Theiler's virus infection and restraint stress. *J. Neuroimmunol.* 151: 103–115.
30. Deng, C., A. Minguela, R. Z. Hussain, A. E. Lovett-Racke, C. Radu, E. S. Ward, and M. K. Racke. 2002. Expression of the tyrosine phosphatase SRC homology 2 domain-containing protein tyrosine phosphatase 1 determines T cell activation threshold and severity of experimental autoimmune encephalomyelitis. *J. Immunol.* 168: 4511–4518.
31. Ryan, K. R., D. McCue, and S. M. Anderton. 2005. Fas-mediated death and sensory adaptation limit the pathogenic potential of autoreactive T cells after strong antigenic stimulation. *J. Leukocyte Biol.* 78: 43–50.
32. Garcia, K. C., C. Radu, J. Ho, R. J. Ober, and E. S. Ward. 2001. Kinetics and thermodynamics of T cell receptor-autoantigen interactions in murine experimental autoimmune encephalomyelitis. *Proc. Natl. Acad. Sci. USA* 98: 6818–6823.
33. Crawford, F., H. Kozono, J. White, P. Marrack, and J. Kappler. 1998. Detection of antigen-specific T cells with multivalent soluble class II MHC covalent peptide complexes. *Immunity* 8: 675–682.
34. Savage, P. A., J. J. Boniface, and M. M. Davis. 1999. A kinetic basis for T cell receptor repertoire selection during an immune response. *Immunity* 10: 485–492.
35. Juedes, A. E., P. Hjelmstrom, C. M. Bergman, A. L. Neild, and N. H. Ruddle. 2000. Kinetics and cellular origin of cytokines in the central nervous system: insight into mechanisms of myelin oligodendrocyte glycoprotein-induced experimental autoimmune encephalomyelitis. *J. Immunol.* 164: 419–426.
36. Kawakami, N., U. V. Nagerl, F. Odoardi, T. Bonhoeffer, H. Wekerle, and A. Flügel. 2005. Live imaging of effector cell trafficking and autoantigen recognition within the unfolding autoimmune encephalomyelitis lesion. *J. Exp. Med.* 201: 1805–1814.
37. Hesse, M. D., A. Y. Karulin, B. O. Boehm, P. V. Lehmann, and M. Tary-Lehmann. 2001. A T cell clone's avidity is a function of its activation state. *J. Immunol.* 167: 1353–1361.
38. Murphy, C. A., C. L. Langrish, Y. Chen, W. Blumenschein, T. McClanahan, R. A. Kastelein, J. D. Sedgwick, and D. J. Cua. 2003. Divergent pro- and anti-inflammatory roles for IL-23 and IL-12 in joint autoimmune inflammation. *J. Exp. Med.* 198: 1951–1957.
39. Langrish, C. L., Y. Chen, W. M. Blumenschein, J. Mattson, B. Basham, J. D. Sedgwick, T. McClanahan, R. A. Kastelein, and D. J. Cua. 2005. IL-23 drives a pathogenic T cell population that induces autoimmune inflammation. *J. Exp. Med.* 201: 233–240.
40. Harrington, L. E., R. D. Hatton, P. R. Mangan, H. Turner, T. L. Murphy, K. M. Murphy, and C. T. Weaver. 2005. Interleukin 17-producing $CD4^+$ effector T cells develop via a lineage distinct from the T helper type 1 and 2 lineages. *Nat. Immunol.* 6: 1123–1132.
41. Park, H., Z. Li, X. O. Yang, S. H. Chang, R. Nurieva, Y. H. Wang, Y. Wang, L. Hood, Z. Zhu, Q. Tian, and C. Dong. 2005. A distinct lineage of CD4 T cells regulates tissue inflammation by producing interleukin 17. *Nat. Immunol.* 6: 1133–1141.
42. Flügel, A., T. Berkowicz, T. Ritter, M. Labeur, D. E. Jenne, Z. Li, J. W. Ellwart, M. Willem, H. Lassmann, and H. Wekerle. 2001. Migratory activity and functional changes of green fluorescent effector cells before and during experimental autoimmune encephalomyelitis. *Immunity* 14: 547–560.
43. Tompkins, S. M., J. Padilla, M. C. Dal Canto, J. P. Ting, L. Van Kaer, and S. D. Miller. 2002. De novo central nervous system processing of myelin antigen is required for the initiation of experimental autoimmune encephalomyelitis. *J. Immunol.* 168: 4173–4183.
44. Kawakami, N., S. Lassmann, Z. Li, F. Odoardi, T. Ritter, T. Ziemssen, W. E. Klinkert, J. W. Ellwart, M. Bradl, K. Krivacic, et al. 2004. The activation status of neuroantigen-specific T cells in the target organ determines the clinical outcome of autoimmune encephalomyelitis. *J. Exp. Med.* 199: 185–197.
45. McGargill, M. A., B. G. Wen, C. M. Walsh, and S. M. Hedrick. 2004. A deficiency in Drak2 results in a T cell hypersensitivity and an unexpected resistance to autoimmunity. *Immunity* 21: 781–791.
46. Willenborg, D. O., S. Fordham, C. C. Bernard, W. B. Cowden, and I. A. Ramshaw. 1996. IFN-γ plays a critical down-regulatory role in the induction and effector phase of myelin oligodendrocyte glycoprotein-induced autoimmune encephalomyelitis. *J. Immunol.* 157: 3223–3227.
47. Ferber, I. A., S. Brocke, C. Taylor-Edwards, W. Ridgway, C. Dinisco, L. Steinman, D. Dalton, and C. G. Fathman. 1996. Mice with a disrupted IFN-γ gene are susceptible to the induction of experimental autoimmune encephalomyelitis (EAE). *J. Immunol.* 156: 5–7.
48. Krakowski, M., and T. Owens. 1996. Interferon γ confers resistance to experimental allergic encephalomyelitis. *Eur. J. Immunol.* 26: 1641–1646.
49. Billiau, A., H. Heremans, F. Vandekerckhove, R. Dijkmans, H. Sobis, E. Meulepas, and H. Carton. 1988. Enhancement of experimental allergic encephalomyelitis in mice by antibodies against IFN-γ. *J. Immunol.* 140: 1506–1510.

50. Lublin, F. D., R. L. Knobler, B. Kalman, M. Goldhaber, J. Marini, M. Perrault, C. D'Imperio, J. Joseph, S. S. Alkan, and R. Korngold. 1993. Monoclonal anti-γ interferon antibodies enhance experimental allergic encephalomyelitis. *Autoimmunity* 16: 267–274.
51. Furlan, R., E. Brambilla, F. Ruffini, P. L. Poliani, A. Bergami, P. C. Marconi, D. M. Franciotta, G. Penna, G. Comi, L. Adorini, and G. Martino. 2001. Intrathecal delivery of IFN-γ protects C57BL/6 mice from chronic-progressive experimental autoimmune encephalomyelitis by increasing apoptosis of central nervous system-infiltrating lymphocytes. *J. Immunol.* 167: 1821–1829.
52. Gran, B., N. Chu, G. X. Zhang, S. Yu, Y. Li, X. H. Chen, M. Kamoun, and A. Rostami. 2004. Early administration of IL-12 suppresses EAE through induction of interferon γ. *J. Neuroimmunol.* 156: 123–131.
53. Chu, C. Q., S. Wittmer, and D. K. Dalton. 2000. Failure to suppress the expansion of the activated CD4 T cell population in interferon γ-deficient mice leads to exacerbation of experimental autoimmune encephalomyelitis. *J. Exp. Med.* 192: 123–128.
54. Ruuls, S. R., L. S. Van Der, K. Sontrop, I. Huitinga, and C. D. Dijkstra. 1996. Aggravation of experimental allergic encephalomyelitis (EAE) by administration of nitric oxide (NO) synthase inhibitors. *Clin. Exp. Immunol.* 103: 467–474.
55. Willenborg, D. O., S. A. Fordham, M. A. Staykova, I. A. Ramshaw, and W. B. Cowden. 1999. IFN-γ is critical to the control of murine autoimmune encephalomyelitis and regulates both in the periphery and in the target tissue: a possible role for nitric oxide. *J. Immunol.* 163: 5278–5286.
56. Willenborg, D. O., M. A. Staykova, and W. B. Cowden. 1999. Our shifting understanding of the role of nitric oxide in autoimmune encephalomyelitis: a review. *J. Neuroimmunol.* 100: 21–35.
57. Fenyk-Melody, J. E., A. E. Garrison, S. R. Brunnert, J. R. Weidner, F. Shen, B. A. Shelton, and J. S. Mudgett. 1998. Experimental autoimmune encephalomyelitis is exacerbated in mice lacking the *NOS2* gene. *J. Immunol.* 160: 2940–2946.
58. Pender, M. P., K. B. Nguyen, P. A. McCombe, and J. F. Kerr. 1991. Apoptosis in the nervous system in experimental allergic encephalomyelitis. *J. Neurol. Sci.* 104: 81–87.
59. Ford, A. L., E. Foulcher, F. A. Lemckert, and J. D. Sedgwick. 1996. Microglia induce CD4 T lymphocyte final effector function and death. *J. Exp. Med.* 184: 1737–1745.
60. Bauer, J., M. Bradl, W. F. Hickley, S. Forss-Petter, H. Breitschopf, C. Linington, H. Wekerle, and H. Lassmann. 1998. T cell apoptosis in inflammatory brain lesions: destruction of T cells does not depend on antigen recognition. *Am. J. Pathol.* 153: 715–724.
61. Bronstein-Sitton, N., L. Cohen-Daniel, I. Vaknin, A. V. Ezernitchi, B. Leshem, A. Halabi, Y. Houri-Hadad, E. Greenbaum, Z. Zakay-Rones, L. Shapira, and M. Baniyash. 2003. Sustained exposure to bacterial antigen induces interferon γ-dependent T cell receptor ζ down-regulation and impaired T cell function. *Nat. Immunol.* 4: 957–964.
62. Zehntner, S. P., C. Brickman, L. Bourbonniere, L. Remington, M. Caruso, and T. Owens. 2005. Neutrophils that infiltrate the central nervous system regulate T cell responses. *J. Immunol.* 174: 5124–5131.
63. Kusmartsev, S. A., Y. Li, and S. H. Chen. 2000. Gr-1$^+$ myeloid cells derived from tumor-bearing mice inhibit primary T cell activation induced through CD3/CD28 costimulation. *J. Immunol.* 165: 779–785.
64. Mazzoni, A., V. Bronte, A. Visintin, J. H. Spitzer, E. Apolloni, P. Serafini, P. Zanovello, and D. M. Segal. 2002. Myeloid suppressor lines inhibit T cell responses by an NO-dependent mechanism. *J. Immunol.* 168: 689–695.
65. Cope, A. P., R. S. Liblau, X. D. Yang, M. Congia, C. Laudanna, R. D. Schreiber, L. Probert, G. Kollias, and H. O. McDevitt. 1997. Chronic tumor necrosis factor alters T cell responses by attenuating T cell receptor signaling. *J. Exp. Med.* 185: 1573–1584.
66. Liu, J., M. W. Marino, G. Wong, D. Grail, A. Dunn, J. Bettadapura, A. J. Slavin, L. Old, and C. C. Bernard. 1998. TNF is a potent anti-inflammatory cytokine in autoimmune-mediated demyelination. *Nat. Med.* 4: 78–83.
67. Kassiotis, G., and G. Kollias. 2001. Uncoupling the proinflammatory from the immunosuppressive properties of tumor necrosis factor (TNF) at the p55 TNF receptor level: implications for pathogenesis and therapy of autoimmune demyelination. *J. Exp. Med.* 193: 427–434.
68. Zakharova, M., and H. K. Ziegler. 2005. Paradoxical anti-inflammatory actions of TNF-α: inhibition of IL-12 and IL-23 via TNF receptor 1 in macrophages and dendritic cells. *J. Immunol.* 175: 5024–5033.
69. Isomaki, P., M. Panesar, A. Annenkov, J. M. Clark, B. M. Foxwell, Y. Chernajovsky, and A. P. Cope. 2001. Prolonged exposure of T cells to TNF down-regulates TCRζ and expression of the TCR/CD3 complex at the cell surface. *J. Immunol.* 166: 5495–5507.
70. Gammon, G., J. Klotz, D. Ando, and E. E. Sercarz. 1990. The T cell repertoire to a multideterminant antigen: clonal heterogeneity of the T cell response, variation between syngeneic individuals, and in vitro selection of T cell specificities. *J. Immunol.* 144: 1571–1577.
71. Rees, W., J. Bender, T. K. Teague, R. M. Kedl, F. Crawford, P. Marrack, and J. Kappler. 1999. An inverse relationship between T cell receptor affinity and antigen dose during CD4$^+$ T cell responses in vivo and in vitro. *Proc. Natl. Acad. Sci. USA* 96: 9781–9786.
72. Maverakis, E., J. Beech, D. B. Stevens, A. Ametani, L. Brossay, P. van den Elsen, R. Mendoza, Q. Thai, L. H. Macias, D. Ethell, et al. 2003. Autoreactive T cells can be protected from tolerance induction through competition by flanking determinants for access to class II MHC. *Proc. Natl. Acad. Sci. USA* 100: 5342–5347.
73. Madakamutil, L. T., I. Maricic, E. Sercarz, and V. Kumar. 2003. Regulatory T cells control autoimmunity in vivo by inducing apoptotic depletion of activated pathogenic lymphocytes. *J. Immunol.* 170: 2985–2992.
74. Sercarz, E. E., and E. Maverakis. 2004. Recognition and function in a degenerate immune system. *Mol. Immunol.* 40: 1003–1008.